

Synthesis of nanostructured copper hexacyanidoferrate and its application in voltammetric detection of salbutamol

Mamta Latwal · Prakash Chandra ·
Shah Raj Ali

Received: 28 April 2014 / Accepted: 18 August 2014 / Published online: 2 September 2014
© Springer Science+Business Media Dordrecht 2014

Abstract Nanostructured copper hexacyanidoferrate has been synthesized and characterized using elemental analysis, atomic absorption spectroscopy, thermal and infrared spectral studies. The transmission electron microscopic studies of the synthesized material showed that it consisted of irregular oval and rod shaped particles with a size range 70–100 nm. Nanostructured copper hexacyanidoferrate modified glassy carbon electrode was characterized by cyclic voltammetry and nanostructured copper hexacyanidoferrate–carbon nanotube composite material modified glassy carbon electrode has been used for electrocatalytic oxidation of salbutamol. The electrode modified with composite material was found to reduce the peak potential of oxidation of salbutamol by nearly 90 mV.

Keywords Nanostructured copper hexacyanidoferrate · Salbutamol · Cyclic voltammetry

1 Introduction

Metal hexacyanidoferrates constitute an important class of inorganic materials which exhibit excellent electron transfer mediator property, high ionic conductivity and mixed valency [1–3]. These materials possess a zeolitic structure which enables them to intercalate alkali metal cations in their cavities in order to maintain electrical

neutrality during the electrochemical redox processes. Due to the above characteristic properties, these materials have been used for the electrochemical detection of a number of biologically important molecules including drugs. Electrodes modified with cobalt hexacyanidoferrate have been used for the detection of NADH [4] and sulfite [5] using cyclic voltammetry. Electrodes modified with nickel hexacyanidoferrate have been used for the development of voltammetric sensors for determining hydrazine [6], ascorbic acid [7], dipyrone [8], and methanol and oxalic acid [9]. Zinc hexacyanidoferrate film has been employed for detecting triglycerides in biological samples [10]. Copper hexacyanidoferrate has also been used in the preparation of modified electrodes which were used as sensors for several compounds. Electrodes modified with copper hexacyanidoferrate have been used for the voltammetric detection of hydrogen peroxide and sulphur oxides [11–13].

Salbutamol is one of the most widely used antiasthmatic drugs. It is used in the treatment of bronchial asthma and other forms of allergic airways disease. The use of this drug is permitted to athletes having asthmatic problems or exercise induced asthma [14]. It is a β_2 adrenergic receptor agonist drug. It causes highly adverse side effects as stimulant and anabolic agent when administered in higher doses than permitted one. Because of this, over dose of this drug is strictly prohibited. Therefore, the determination of salbutamol is an important issue. Salbutamol has been determined in human plasma and urine samples using high performance liquid chromatography (HPLC) method [15]. However, electrochemical methods are superior to HPLC methods due to their extreme simplicity, short analysis time, low cost instrumentation, high sensitivity and specificity. Therefore, researchers have shown growing interest in the development of electrochemical methods for the

M. Latwal
Department of Chemistry, University of Petroleum & Energy
Studies, Dehradun 248 007, Uttarakhand, India

P. Chandra · S. R. Ali (✉)
Department of Chemistry, Kumaun University,
Nainital 263 002, Uttarakhand, India
e-mail: shahrajali@gmail.com

determination of salbutamol. Only a few reports have been published in this particular electrochemical detection of salbutamol. Goyal et al. [16] studied the effect of graphite and metallic impurities of C₆₀ fullerene on the determination of salbutamol in biological fluids using Osteryoung square wave voltammetry. Karuwan et al. [17] employed carbon nanotube electrode in microfabricated flow injection device for determining salbutamol. Salbutamol sulphate in pharmaceutical preparations was determined by Abachi and Hadi [18] using continuous/stopped flow injection method. Salbutamol has also been determined using cyclic voltammetry by Wei et al. [19]. In this contribution, we describe the synthesis of nanostructured copper hexacyanidoferrate (NsCuHcFe) and its application in voltammetric detection of salbutamol. Previously, we have reported the synthesis of nanocubic cadmium hexacyanidoferrate and its application in voltammetric determination of morphine [20]. Also, we have reported the synthesis of some other nanostructured hexacyanidoferrates and their catalytic properties [21, 22].

2 Experimental

2.1 Chemicals

K₃[Fe(CN)₆]·H₂O, Cu(NO₃)₂·6H₂O, CH₃COCH₃, KCl and KNO₃ were purchased from Merck. C-TAB and CNT were purchased from Hi Media and Intelligent Materials Pvt. Ltd., respectively. Salbutamol manufactured by Sigma Aldrich was used. All the chemicals were used as received. Doubly distilled water was used throughout the experiments.

2.2 Synthesis of NsCuHcFe

NsCuHcFe was synthesized using a reported method [23]. In brief, 600 ml aqueous solution of 0.001 M copper nitrate containing equimolar amount of C-TAB was slowly added drop wise to 400 ml aqueous solution of 0.001 M potassium hexacyanidoferrate containing equimolar amount of KCL. The reaction mixture was kept stirred at room temperature using a magnetic stirrer. After complete mixing, the reaction mixture was vigorously agitated for 5 min which produced an aqueous suspension of NsCuHcFe. It was filtered using a Buchner funnel and the solid material was washed thoroughly with distilled water. The solid precipitate so obtained was dried overnight, crushed and then sieved with mesh size 100.

2.3 Characterization of synthesized material

The percentage of C, H and N in the synthesized material was determined using an Elementar Vario EL-III CHNS

analyzer. The percentage of Cu and Fe was determined using a Perkin Elmer atomic absorption spectrophotometer. TG/DT analysis was carried out using a Perkin Elmer analyzer system. IR spectral studies were carried out using a Perkin Elmer spectrophotometer. The X-ray diffraction data was recorded on a Philips PW-1140/90 X-ray diffractometer. The TEM image of the synthesized NsCuHcFe was recorded using a JEOL 1011 instrument.

2.4 Modification of electrode

The glassy carbon electrode (GCE, 3 mm diameter) was cleaned by polishing with 1 μm α-alumina paste on polishing plate and rinsed with distilled water before use. NsCuHcFe was dispersed in acetone to prepare a colloidal emulsion. This solution was agitated in bath sonicator for 30 min. Approximately 3 μl of this emulsion was taken using a micropipette and it was cast on unit area of GCE surface. After evaporation of acetone, a thin and robust film of NsCuHcFe was formed on GCE surface. The nanostructured copper hexacyanidoferrate modified glassy carbon electrode (NsCuHcFe/GCE) so prepared was then rinsed thoroughly with distilled water and subjected to electrochemical characterization using cyclic voltammetry. In similar manner, nanostructured copper hexacyanidoferrate-carbon nanotube composite modified glassy carbon electrode (NsCuHcFe-CNT/GCE) was also prepared.

2.5 Electrochemical studies

The electrochemical experiments were performed using a cyclic voltammeter (Paras Industrial Products, Roorkee). An electrochemical cell having three conventional electrodes in a small vial container was used. Ag/AgCl_{sat}, Pt wire and GCE were used as reference electrode, auxiliary electrode and working electrode, respectively. All electrochemical studies were carried out at 25 ± 0.2 °C. All three electrodes were dipped in the electrochemical cell containing 0.1 M KNO₃.

3 Results and discussions

3.1 Synthesis of NsCuHcFe

The mixing of dilute solution of Cu²⁺ ions into a dilute solution of [Fe(CN)₆]^{3−} ions under the reaction conditions used herein resulted in the formation of NsCuHcFe. The C-TAB molecules added during the reaction act as stabilizer for maintaining uniformity in shape of nanoparticles and also prevent their agglomeration. The percentage of all the elements present in the synthesized material is given in

Table 1 Elemental analyses and TG/DT analyses of NsCuHcFe

S. no.	C %	N %	H %	Cu %	Fe %	H ₂ O %
Theoretical values	19.93	23.25	1.66	26.38	15.46	14.33
Observed values	19.69	22.98	1.43	26.59	15.72	13.98

Table 1. The observed values of elemental percentage and water loss in TG/DT analysis were found to be approximately equal to the calculated values for NsCuHcFe. The molecular formula of the synthesized material so obtained was $\text{Cu}_3[\text{Fe}^{\text{III}}(\text{CN})_6]_2 \cdot 6\text{H}_2\text{O}$. The TG/DT curve of synthesized NsCuHcFe is shown in Fig. 1. It shows approximately 14 % mass loss on heating up to 160 °C. This mass loss corresponded to the loss of six water molecules from the synthesized material. These results were consistent with the earlier reports by Avila et al. [24]. They have reported that metal hexacyanidoferrates lose water content on thermal decomposition up to 160 °C. The synthesis of copper hexacyanidoferrate was confirmed by X-ray diffraction data as the values of interplanar spacing (*d*) and relative intensity were found in good agreement with reported values. The X-ray diffraction data are shown in Table 2. Ayers and coworkers have synthesized copper hexacyanidoferrates with molecular formulae $\text{Cu}_{1.5}[\text{Fe}(\text{CN})_6] \cdot 6\text{H}_2\text{O}$ and $\text{Cu}_3[\text{Fe}(\text{CN})_6] \cdot 4\text{H}_2\text{O}$ [25, 26]. They have also reported face centered cubic lattice structures of synthesized complexes. TEM studies revealed that the synthesized material consists of roughly spherical, oval and rod shaped particles in the size range 70–100 nm. The TEM image of NsCuHcFe is shown in Fig. 2. It is clear

from the image that there is no agglomeration in the synthesized nanomaterial. The IR spectrum of synthesized NsCuHcFe showed a sharp peak at $2,102\text{ cm}^{-1}$ which is characteristic of $\text{C}\equiv\text{N}$ group present in $-\text{Fe}(\text{III})-\text{CN}-\text{Cu}(\text{II})-$ unit and another peak at 594 cm^{-1} which is characteristic of Fe–C stretching. A broad band in the range of $3,300\text{--}3,600\text{ cm}^{-1}$ was also observed which is characteristic of H-bonding that takes place between water molecules present in the interstitial sites of the crystal lattice of NsCuHcFe. These results were consistent with our previous studies [20–22].

3.2 Characterization of NsCuHcFe/GCE

The characterization of NsCuHcFe/GCE was done using a cyclic voltammeter and all the voltammograms were recorded at room temperature. Cyclic voltammogram of bare GCE was recorded in 0.1 M KNO_3 solution at a scan rate 50 mV/s and is shown in Fig. 3. It was observed that there was no peak due to the electrolyte. The electrochemical behaviour of synthesized NsCuHcFe was studied by recording the cyclic voltammogram of NsCuHcFe/GCE in 0.1 M KNO_3 solution at scan rate 20, 40, 60, 80 and 100 mV/s. The voltammogram is shown in Fig. 4. It shows the formation of a reversible redox couple whose formal potential was found to be nearly 675 mV. The values of anodic peak potential (E_a), cathodic peak potential (E_c), formal potential (E°), and potential separation (ΔE) between E_a and E_c in voltammograms of NsCuHcFe/GCE at different scan rate are shown in Table 3. From this table, it is clear that on increasing the scan rate, the value of E_a

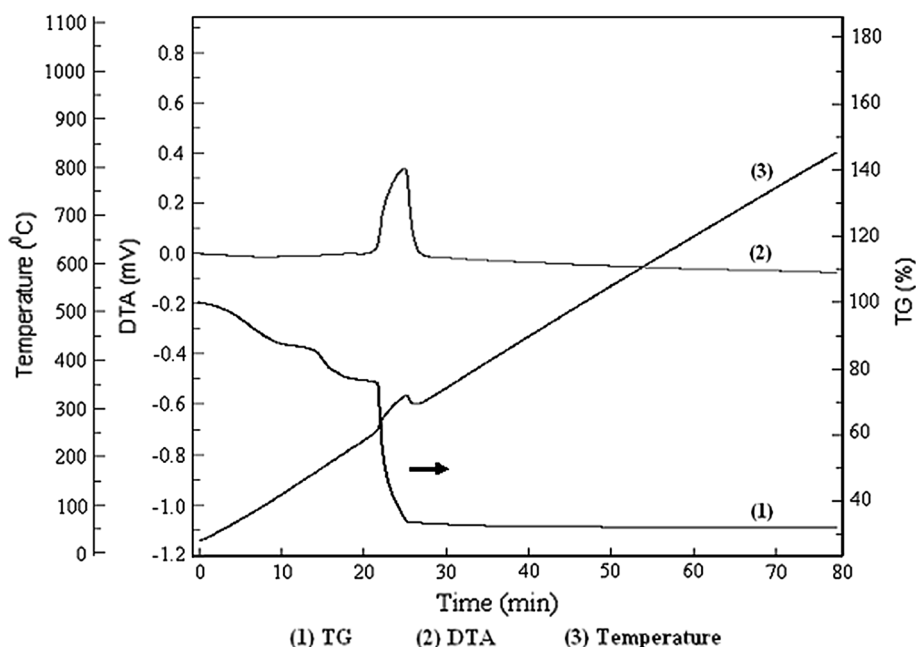
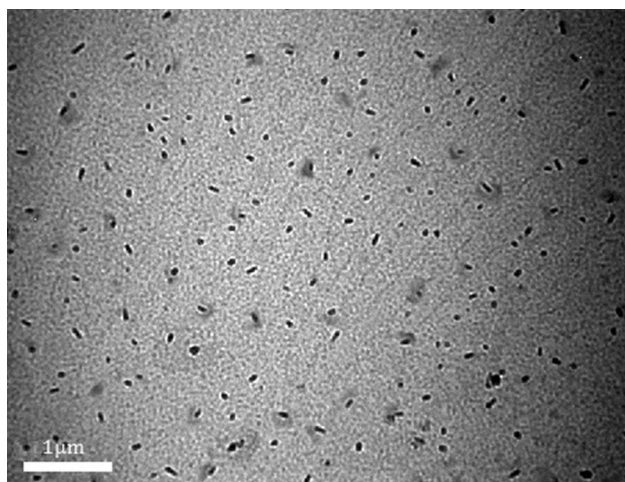
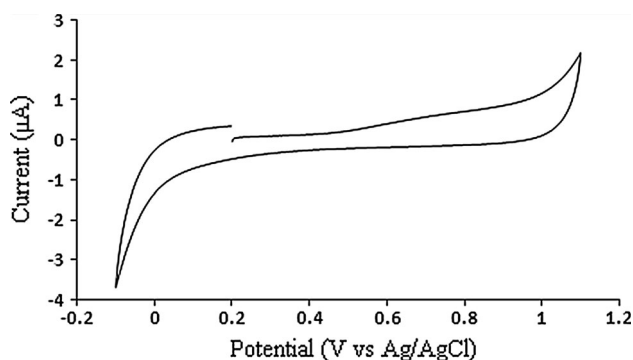
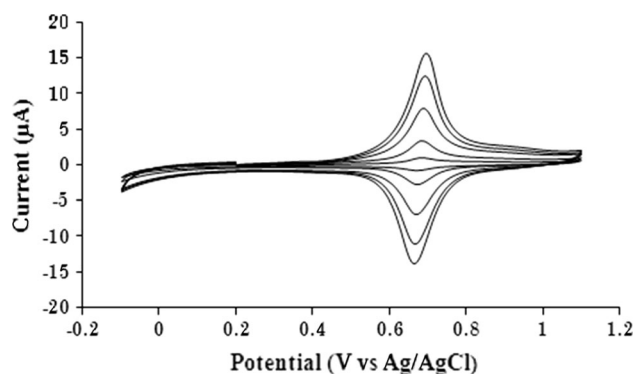
Fig. 1 TG/DT spectra of NsCuHcFe

Table 2 X-ray diffraction data of NsCuHcFe

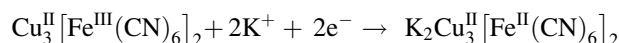
d (Å)	5.00 (5.00) ^a	3.54 (3.55)	2.50 (2.50)	2.24 (2.23)	2.04 (2.04)	1.77 (1.76)	1.58 (1.58)
hkl	100 (100)	72 (75)	48 (50)	21 (25)	23 (20)	17 (15)	11 (10)

^a Bracket values indicate the reported data**Fig. 2** TEM image of NsCuHcFe**Fig. 3** CV of KNO₃ using bare GCE at a scan rate of 50 mV/s

increases but the values of E_c decreases. Therefore, the value of ΔE increases significantly on increasing the scan rate. The value of ΔE was found to increase from 10 to 50 mV on increasing the scan rate from 20 to 100 mV/s. The value of ΔE should be equal to 56 mV or less than 56 mV for the reversibility of the system. In present case the values of ΔE were found to be less than 56 mV which shows the reversibility of the system. The Fig. 4 shows that the peak current increases significantly on increasing the scan rate while the formal potential remains constant. The voltammograms of NsCuHcFe/GCE were almost similar to the earlier reported results for CuHcFe/GCE [27]. The electrochemical process of redox couple formation can be explained on the basis of following equation:

**Fig. 4** CV of NsCuHcFe/GCE in 0.1 M KNO₃ at scan rate 20, 40, 60, 80 and 100 mV/s (inner to out)**Table 3** The values of E_a , E_c , E° and ΔE of NsCuHcFe/GCE at different scan rates

S. no.	Scan rate (mV/s)	E_a (mV)	E_c (mV)	E° (mV)	ΔE (mV)
1.	20	680	670	675	10
2.	40	685	665	675	20
3.	60	690	660	675	30
4.	80	695	655	675	40
5.	100	700	650	675	50



In the above reaction, $\text{K}_2\text{Cu}_3^{\text{II}}[\text{Fe}^{\text{II}}(\text{CN})_6]_2$ represents a combined form of $\text{Cu}_2^{\text{II}}[\text{Fe}^{\text{II}}(\text{CN})_6]$ and $\text{K}_2\text{Cu}^{\text{II}}[\text{Fe}^{\text{II}}(\text{CN})_6]$. The formation of $\text{K}_2\text{Cu}_3^{\text{II}}[\text{Fe}^{\text{II}}(\text{CN})_6]_2$ species in thin film has been reported by Rutkowska et al. [28].

3.2.1 Effect of nature of electrolyte

The effect of nature of electrolyte on the electrochemical behavior of NsCuHcFe/GCE was studied by recording the voltammograms in an electrolyte solution with different alkali metal cations. The cyclic voltammograms of NsCuHcFe/GCE were recorded in 0.1 M LiNO₃, 0.1 M NaNO₃ and 0.1 M KNO₃ solutions at scan rate 50 mV/s and the results are shown in Fig. 5. The values of E_a , E_c , E° and ΔE for NsCuHcFe/GCE have been shown in Table 4. From a comparative study of these voltammograms it is clear that a well-defined redox peak appears in case of K⁺ ion containing electrolyte. The electrolytes containing Na⁺

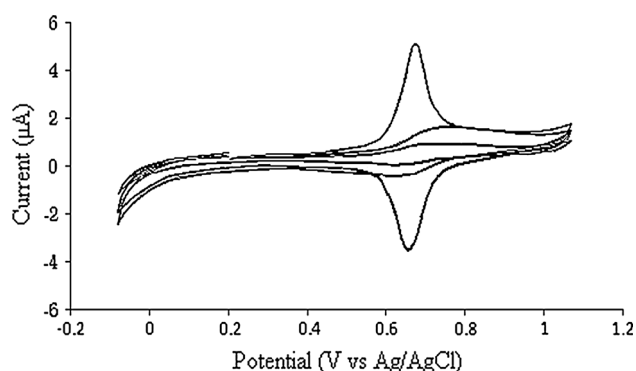


Fig. 5 CV of NsCuHcFe/GCE in LiNO_3 , NaNO_3 and KNO_3 (inner to out) at scan rate 50 mV/s

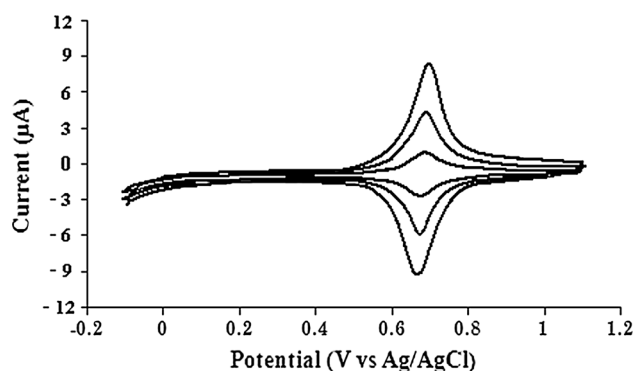


Fig. 6 CV of NsCuHcFe/GCE in 0.05 M, 0.1 M, and 0.5 M KNO_3 (inner to out) at scan rate 50 mV/s

Table 4 The values of E_a , E_c , E° and ΔE of NsCuHcFe/GCE in different electrolyte at scan rate of 50 mV/s

S. no.	Electrolyte (0.1 M)	E_a (mV)	E_c (mV)	E° (mV)	ΔE (mV)
1.	KNO_3	690	660	675	30
2.	NaNO_3	760	610	685	150
3.	LiNO_3	750	620	685	130

and Li^+ ions showed broad and ill-defined peaks. Meanwhile, the highest peak current was also found in the former case. In an aqueous solution, alkali metal ions exist in hydrated form and they must undergo dehydration before their insertion into crystals of metal hexacyanidoferrate. Lundgren and Murray have proposed that the electrochemical behavior of metal hexacyanidoferrates in LiNO_3 , NaNO_3 and KNO_3 electrolytes is dependent upon the ease of dehydration of alkali metal ions [29]. The hydration energy of K^+ , Li^+ and Na^+ has been reported as 3.34, 5.07 and 4.08 mV, respectively [29]. Therefore, hydrated K^+ undergoes dehydration more easily than Li^+ and Na^+ . Thus, K^+ ions insert in the cavities of NsCuHcFe most easily and increase the peak current as well. Therefore, KNO_3 solution was used for further studies. Similar results were found in our previous studies [20].

3.2.2 Effect of electrolyte concentration

The effect of electrolyte concentration on the electrochemical behavior of NsCuHcFe/GCE was also studied. Figure 6 shows the cyclic voltammograms of NsCuHcFe/GCE in 0.50 M KNO_3 , 0.10 M KNO_3 and 0.05 M KNO_3 solution at a scan rate of 50 mV/s. The values of E_a , E_c , E° , and ΔE corresponding to different concentration of KNO_3 have been shown in Table 5. These results showed that on decreasing the concentration of KNO_3 from 0.5 M to

Table 5 The values of E_a , E_c , E° and ΔE of NsCuHcFe/GCE in different concentration of KNO_3 at scan rate of 50 mV/s

S no.	KNO_3 Conc. (M)	E_a (mV)	E_c (mV)	E° (mV)	ΔE (mV)
1.	0.05	682	666	674	16
2.	0.1	690	660	675	30
3.	0.5	702	656	679	46

0.05 M, the redox peak goes on shifting towards negative direction of potential scale. The 0.1 M KNO_3 solution exhibited a well-defined redox peak. Therefore, 0.1 M concentration of KNO_3 was selected for subsequent studies. The same concentration was found optimum in our previous studies as well [20].

3.2.3 Effect of ratio of CNT on NsCuHcFe-CNT/GCE

The effect of CNT on electrochemical behavior of NsCuHcFe was studied by comparing the voltammograms of NsCuHcFe/GCE, CNT/GCE, and NsCuHcFe-CNT/GCE recorded in 0.1 M KNO_3 at a scan rate of 50 mV/s. Figure 7 shows the voltammogram of CNT/GCE which gave no peak. Figure 8 shows the voltammogram of NsCuHcFe/GCE (inner) and NsCuHcFe-CNT/GCE (outer). On comparing the voltammogram of NsCuHcFe/GCE with the voltammogram of NsCuHcFe-CNT/GCE, it was found that the peak potential was nearly the same in each case. It indicates that the addition of CNT did not affect the peak potential for inter-conversion of $\text{Cu}^{\text{II}}[\text{Fe}^{\text{III}}(\text{CN})_6]/\text{Cu}^{\text{II}}[\text{Fe}^{\text{II}}(\text{CN})_6]$. However, the peak current for NsCuHcFe-CNT/GCE was found to be three times more than that of NsCuHcFe/GCE. It showed a good synergic effect in NsCuHcFe-CNT composite film which may be associated with the excellent electron-transfer property of CNT which is well-known.

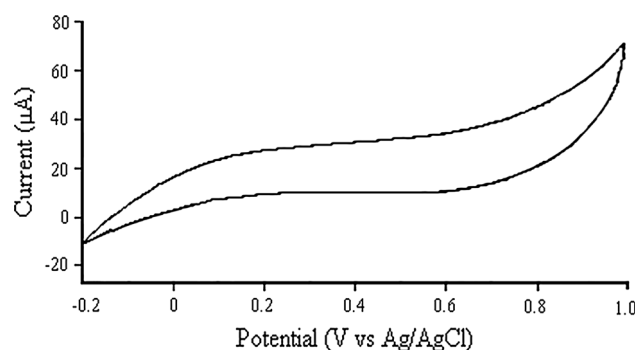


Fig. 7 CV of CNT/GCE in 0.1 M KNO₃ at scan rate 50 mV/s

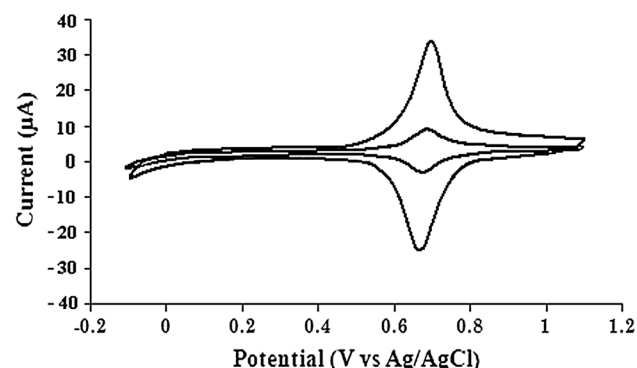


Fig. 8 CV of NsCuHcFe/GCE (inner) and NsCuHcFe-CNT/GCE (outer) in 0.1 M KNO₃ at scan rate 50 mV/s

Further, the effect of different ratios of NsCuHcFe to CNT on the electrochemical behavior of NsCuHcFe-CNT/GCE was also investigated in terms of the voltammograms of NsCuHcFe-CNT/GCE in 0.1 M KNO₃ at a scan rate of 50 mV/s using NsCuHcFe:CNT = 4:1, 4:2, 4:3, 4:4 and 4:5. The voltammograms are shown in Fig. 9. These results indicate a significant increase in peak current of NsCuHcFe on increasing the amount of CNT and it was found to be optimal when the amounts of both the components were equal.

3.2.4 Electrocatalytic potential of NsCuHcFe-CNT/GCE for oxidation of salbutamol

The electrocatalytic potential of NsCuHcFe-CNT/GCE for the oxidation of salbutamol was studied using NsCuHcFe-CNT/GCE at pH 7.0 using 0.1 M KNO₃ + 2.5×10^{-2} M phosphate buffer solution (PBS) as a supporting electrolyte. The addition of 2.5×10^{-2} M PBS to 0.1 M KNO₃ solution does not affect the peak potential of metal hexacyanidoferrates [30]. We have chosen the neutral pH for the electro-oxidation of this drug because most of the physiochemical processes in human body take place at the

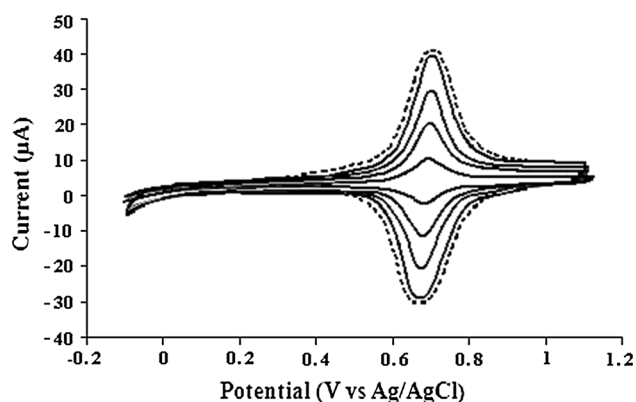


Fig. 9 CV of NsCuHcFe-CNT/GCE with increasing amount of CNT (inner to out) and fixed amount of NsCuHcFe in 0.1 M KNO₃ at scan rate 50 mV/s

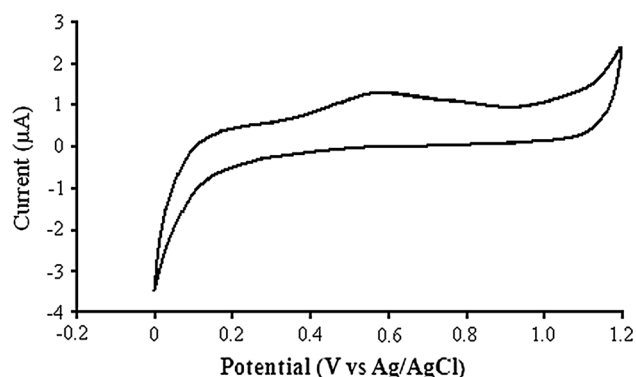


Fig. 10 CV of bare GCE in 0.1 M KNO₃ + 2.5×10^{-2} M PBS containing 20 μM salbutamol at scan rate 50 mV/s

neutral pH. Approximately 20 μM salbutamol was introduced into 0.1 M KNO₃ + 2.5×10^{-2} M PBS and the cyclic voltammogram was recorded using bare GCE at a scan rate of 50 mV/s. This voltammogram is shown in Fig. 10. It showed a broad anodic peak at 590 mV which may be attributed to the oxidation potential of salbutamol on bare GCE. After this, a voltammogram of salbutamol (20 μM) in 0.1 M KNO₃ + 2.5×10^{-2} M PBS was also recorded using NsCuHcFe/GCE at a scan rate of 50 mV/s and the voltammogram is shown in Fig. 11. It showed one anodic peak at 500 mV in addition to that of NsCuHcFe and this additional peak was due to the oxidation of salbutamol in case of NsCuHcFe/GCE. Further, cyclic voltammogram of salbutamol in 0.1 M KNO₃ + 5×10^{-2} M PBS using NsCuHcFe-CNT/GCE at the same scan rate was recorded which also showed additional peak for the oxidation of salbutamol at 500 mV only. The voltammograms of salbutamol using its different concentrations (5, 10, 15, 20 and 25 μM) on NsCuHcFe-CNT/GCE are shown in Fig. 12. The Figs. 10, 11 and 12 indicate that the difference of the peak potential of salbutamol using bare GCE and

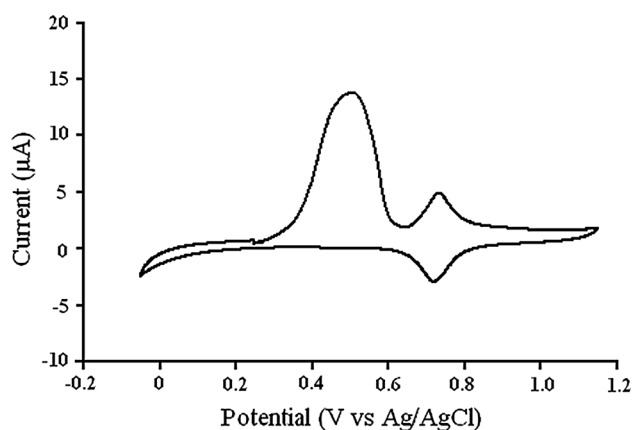


Fig. 11 CV of NsCuHcFe/GCE in 0.1 M $\text{KNO}_3 + 2.5 \times 10^{-2}$ M PBS containing 20 μM salbutamol at scan rate 50 mV/s

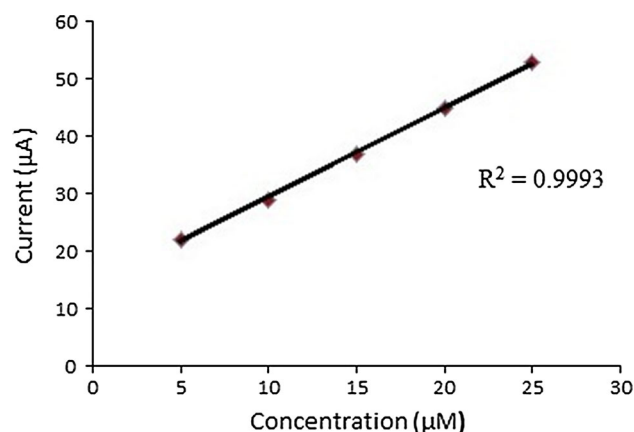


Fig. 13 Plot for peak current versus concentration of salbutamol

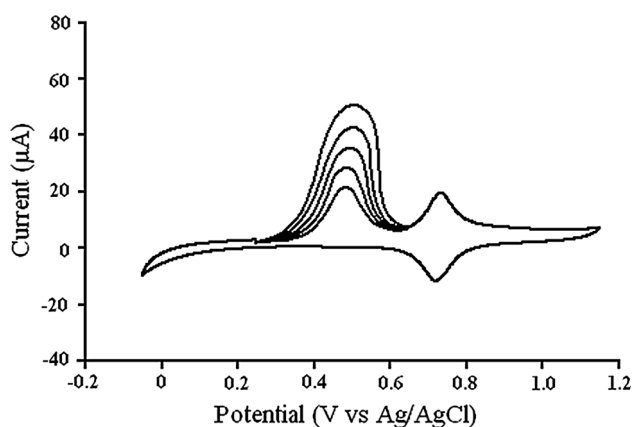


Fig. 12 CV of NsCuHcFe-CNT/GCE in 0.1 M $\text{KNO}_3 + 2.5 \times 10^{-2}$ M PBS with salbutamol concentration 5, 10, 15, 20 and 25 μM (inner to out) at scan rate 50 mV/s

NsCuHcFe/GCE or NsCuHcFe-CNT/GCE was 90 mV which was equal to the reduction in the peak potential of salbutamol. Thus, NsCuHcFe/GCE as well as NsCuHcFe-CNT/GCE reduced the peak potential of salbutamol by 90 mV. However, Figs. 11 and 12 showed that the peak current corresponding to 20 μM salbutamol was 15 μA in case of NsCuHcFe/GCE and it was 45 μA in case of NsCuHcFe-CNT/GCE. It indicates that the addition of CNT increases the peak current corresponding to salbutamol oxidation three times. Thus, the addition of CNT showed the synergic effect in term of peak current only. The peak current corresponding to salbutamol was significantly higher in the case of NsCuHcFe-CNT/GCE than that on bare GCE. The values of peak current corresponding to salbutamol oxidation using 5, 10, 15, 20 and 25 μM concentration of salbutamol was found to be 22, 29, 37, 45 and 53 μA , respectively. The values of peak current for the anodic peaks were plotted against the corresponding

salbutamol concentrations and the plot is shown in Fig. 13. It shows that the value of peak current increases linearly with increase in the concentration of salbutamol. This observation was in good agreement with the results reported by Goyal et al. [16]. The linear plot exhibited a correlation coefficient of 0.9993 ($n = 5$). It was found that NsCuHcFe-CNT/GCE exhibited a significant increase in oxidation peak current with increase in the concentration of salbutamol. The oxidation process of salbutamol is generally attributed to the oxidation of the phenolic hydroxy group, which can be observed in both acidic and basic medium [31]. The stability of NsCuHcFe-CNT/GCE for its electrocatalytic potential for salbutamol was studied and it was found that there was no significant loss in electrocatalytic activity of NsCuHcFe-CNT/GCE up to 10 days. However, after 15 days its response current was 70 % of the initial response for 20 μM salbutamol. These results indicate that the NsCuHcFe-CNT/GCE exhibits good electrocatalytic activity for the oxidation of salbutamol molecule.

4 Conclusions

Copper hexacyanidoferrate nanostructures consisting of irregular oval and rod shaped particles with 70–100 nm size can be synthesized using a simple method described herein. The C-TAB can act as a good stabilizer for the synthesized nanostructures. The electrochemical characterization of NsCuHcFe/GCE in 0.1 M KNO_3 solution showed that the peak current increases significantly on increasing the scan rate from 20 to 100 mV/s. The formal potential of NsCuHcFe/GCE in 0.1 M KNO_3 remains unaffected on increasing the scan rate. The addition of CNT to NsCuHcFe increased the peak current only without affecting the peak potential of NsCuHcFe. The NsCuHcFe-

CNT/GCE reduced the peak potential of salbutamol by 90 mV. It also exhibited a linear relationship between salbutamol concentration up to 25 μM and corresponding peak current.

Acknowledgments This research work was sponsored by Council of Scientific and Industrial Research (CSIR), New Delhi.

References

1. Sinha S, Humphery BD, Bocarsly AB (1984) The reaction of nickel electrode surfaces with metal-cyanide anionic complexes: the formation of precipitated surfaces. *Inorg Chem* 23:203–212
2. Kulesza PJ, Galus Z (1992) Mixed-valence electron hopping, redox conduction and migration effects in solid-state electrochemistry of transition metal hexacyanoferrates. *J Electroanal Chem* 323:261–274
3. Chen SM, Lu MF, Lin KH (2005) Preparation and characterization of ruthenium oxide/hexacyanoferrate and ruthenium hexacyanoferrate mixed films and their electrocatalytic properties. *J Electroanal Chem* 579:163–174
4. Zhang Q, Zhu R, Kang Q, Lu W, Zhang H, Pan D (2012) Water-miscible room-temperature ionic liquid-cobalt hexacyanoferrate gel modified electrode for electrocatalytic oxidation of NADH. *Int J Electrochem Sci* 7:8185–8193
5. Cumba LR, Bicalho UdeO, do Carmo DR (2012) Voltammetric studies of cobalt hexacyanoferrate formed on the titanium (IV) phosphate surface and its application to the determination of sulfite. *Int J Electrochem Sci* 7:2123–2135
6. Sophia SJ, Devi S, Pandian K (2012) Electrocatalytic oxidation of hydrazine based on NiHCF@TiO_2 core-shell nanoparticles modified GCE. *Int J Electrochem Sci* 7:6580–6598
7. Wang Y, Rui Y, Li F, Li M (2014) Electrodeposition of nickel hexacyanoferrate/layered double hydroxide hybrid film on the gold electrode and its application in the electroanalysis of ascorbic acid. *Electrochim Acta* 117:398–404
8. Cumba LR, UdeO Bicalho, Silvestrini DR, do Carmo DR (2012) Preparation and voltammetric study of a composite titanium phosphate/nickel hexacyanoferrate and its application in dipyrone determination. *Int J Chem* 4:66–78
9. Hathoot AA, El-Maghrabi S, Abdel-Azzem M (2011) Electrochemical and electrocatalytic properties of hybrid films composed of conducting polymer and metal hexacyanoferrates. *Int J Electrochem Sci* 6:637–649
10. Narang J, Chauhan N, Pundir CS (2013) Construction of triglyceride biosensor based on nickel oxide-chitosan/zinc oxide/zinc hexacyanoferrate film. *Int J Biol Macromol* 60:45–51
11. Tsai T, Chen T, Chen S (2011) Copper nanoparticles with copper hexacyanoferrate and poly(3,4-ethylenedioxythiophene) hybrid film modified electrode for hydrogen peroxide detection. *Int J Electrochem Sci* 6:4628–4637
12. Chen SM, Chan CM (2003) Preparation, characterization, and electrocatalytic properties of copper hexacyanoferrate film and bilayer film modified electrodes. *J Electroanal Chem* 543:161–173
13. Wu H, Hu J, Li H, Li H (2013) A novel photo-electrochemical sensor for determination of hydroquinone based on copper hexacyanoferrate and platinum films modified n-silicon electrode. *Sens Act B* 182:802–808
14. Pichon A, Venisse N, Krupka E, Perault-Pochat MC, Denjean A (2006) Urinary and blood concentrations of beta2-agonists in trained subjects: comparison between routes of use. *Int J Sports Med* 27:187–192
15. Zhang XZ, Gan YR, Zhao FN (2004) Determination of salbutamol in human plasma and urine by high-performance liquid chromatography with a coulometric electrode array system. *J Chromatogr Sci* 42:263–267
16. Goyal RN, Kaur D, Singh SP, Pandey AK (2008) Effect of graphite and metallic impurities of C60 fullerene on determination of salbutamol in biological fluids. *Talanta* 75:63–69
17. Karuwan C, Wisitsoraat A, Matusos T, Phokharatkul D, Sappat A et al (2009) Flow injection based microfluidic device with carbon nanotube electrode for rapid salbutamol detection. *Talanta* 79:995–1000
18. Abachi MQA, Hadi H (2012) Determination of salbutamol sulphate in pharmaceutical preparations using continuous/stopped flow injection method. *Int J Res Pharm Biomed Sci* 3:1189–1199
19. Wei Y, Zhang Q, Shao C, Li C, Zhang L, Li X (2012) Voltammetric determination of salbutamol on a glassy carbon electrode coated with a nanomaterial thin film. *J Anal Chem* 65:398–403
20. Ali SR, Chandra P, Latwal M, Jain SK, Bansal VK (2011) Growth of cadmium hexacyanidoferrate (III) nanocubes and its application in voltammetric determination of morphine. *Bull Chem Soc Jpn* 84:1355–1361
21. Ali SR, Bansal VK, Khan AA, Jain SK, Ansari MA (2009) Growth of zinc hexacyanoferrate nanocubes and their potential as heterogeneous catalyst for solvent-free oxidation of benzyl alcohol. *J Mol Catal A* 303:60–64
22. Ali SR, Chandra P, Latwal M, Jain SK, Bansal VK, Singh SP (2011) Synthesis of nickel hexacyanoferrate nanoparticles and their potential as heterogeneous catalysts for the solvent-free oxidation of benzyl alcohol. *Chin J Catal* 32:1844–1849
23. Qu F, Yang M, Lu Y, Shen G, Yu R (2006) Amperometric determination of bovine insulin based on synergic action of carbon nanotubes and cobalt hexacyanoferrate nanoparticles stabilized by EDTA. *Anal Bioanal Chem* 386:228–234
24. Avila M, Reguera L, Rodriguez-Hernandez J, Balmaseda J, Reguera E (2008) Porous framework of $\text{T}_2[\text{Fe}(\text{CN})_6] \cdot x\text{H}_2\text{O}$ with $\text{T} = \text{Co}, \text{Ni}, \text{Cu}, \text{Zn}$, and H_2 storage. *J Solid State Chem* 181:2899–2907
25. Ayers et al (1971) Private Communication CAS Number: 32105-67-2
26. Ayers et al (1986) Private Communication CAS Number: 32492-17-4
27. Yang M, Jiang J, Yang Y, Chen X, Shen G, Yu R (2006) Carbon nanotube/cobalt hexacyanoferrate nanoparticle-biopolymer system for the fabrication of biosensors. *Biosens Bioelectron* 21:1791–1797
28. Rutkowska IA, Stroka J, Galus Z (2008) Electrochemical properties of modified copper-thallium hexacyanoferrate electrode in the presence of different univalent cations. *Electrochim Acta* 53:3870–3878
29. Lundgren CA, Murray RW (1988) Observations on the composition of Prussian blue films and their electrochemistry. *Inorg Chem* 27:933–939
30. Xun Z, Cai C, Xing W, Lu T (2003) Electrocatalytic oxidation of dopamine at a cobalt hexacyanoferrates modified glassy carbon electrode prepared by a new method. *J Electroanal Chem* 545:19–27
31. Bishop E, Hussein W (1984) Anodic voltammetry of dopamine, noradrenaline and related compounds at rotating disc electrodes of platinum and gold. *Analyst* 109:627–632